Naval Research Laboratory
Stennis Space Center, MS 39529-5004

A Semi-Empirical Longshore Current Model

DENNIS L. LUNDBERG
K. TODD HOLLAND
JOHN CASEY CHURCH

Mapping, Charting, and Geodesy Branch
Marine Geosciences Division

October 24, 1997

19971118 024

DTIC QUALITY INSPECTED 2

REPORT DOCUMENTATION PAGE

Form Approved
OBM No. 0704-0188

1. AGENCY USE ONLY *(Leave blank)*	2. REPORT DATE October 24, 1997	3. REPORT TYPE AND DATES COVERED Final

4. TITLE AND SUBTITLE

A Semi-Empirical Longshore Current Model

6. AUTHOR(S)

Dennis L. Lundberg, K. Todd Holland, and John Casey Church

5. FUNDING NUMBERS

Job Order No. 574662008
Program Element No. 0602435N
Project No. Core
Task No.
Accession No.

7. PERFORMING ORGANIZATION NAME(S) AND ADDRESS(ES)

Naval Research Laboratory
Marine Geosciences Division
Stennis Space Center, MS 39529-5004

8. PERFORMING ORGANIZATION REPORT NUMBER

NRL/MR/7442--97-8066

9. SPONSORING/MONITORING AGENCY NAME(S) AND ADDRESS(ES)

Office of Naval Research
800 N. Quincy St.
Arlington, VA 22217-5660

10. SPONSORING/MONITORING AGENCY REPORT NUMBER

11. SUPPLEMENTARY NOTES

12a. DISTRIBUTION/AVAILABILITY STATEMENT

Approved for public release; distribution unlimited

12b. DISTRIBUTION CODE

13. ABSTRACT *(Maximum 200 words)*

A semi-empirical longshore current model has been developed that is not reliant upon bathymetry. The model inputs are wave breaker height, wave breaker angle, and the surf width. The output is a cross-shore profile of the longshore current that is consistent with field observations for both planar and barred beaches. Since the model inputs are those that can be readily determined by observation, this model has utility for forward deployed operational forces that may not have ready access to more sophisticated models and measurement techniques. The concept of wave radiation stress was used to provide the driving force in the model. The model was developed and tested from data gathered at Duck, NC during the DELILAH experiment in October, 1990. The beach at Duck had an offshore bar during the data collection. The average absolute deviation of the model compared to the measured data was 19%. The model will require further testing to verify its general application for both plane and barred beaches.

14. SUBJECT TERMS

longshore current, surfzone, mine warfare, amphibious warfare

15. NUMBER OF PAGES 39

16. PRICE CODE

17. SECURITY CLASSIFICATION OF REPORT	18. SECURITY CLASSIFICATION OF THIS PAGE	19. SECURITY CLASSIFICATION OF ABSTRACT	20. LIMITATION OF ABSTRACT
Unclassified	Unclassified	Unclassified	SAR

A SEMI-EMPIRICAL LONGSHORE CURRENT MODEL

INTRODUCTION

The impetus for this study was to develop a longshore current model that could be applied using simple and observable inputs. One scenario for its application would be to support Naval operations in remote coastal regions where the only data available of the surf conditions are those that can be visually seen (e.g. wave height, wave angle, and surf width) such that the cross-shore profile of the longshore current could be predicted. The data used in the development of this model were taken at the U.S. Army Corps of Engineers Field Research Facility located at Duck, NC which is typically a barred beach.

Previous Work

The concept of radiation stress was introduced in a series of papers by Longuet-Higgins and Stewart (1960, 1961, 1962, 1963, 1964) and is fundamental to all modern approaches to modeling the longshore current. This excess transfer of momentum due to waves has an alongshore component that can be shown to force the longshore current.

Longuet-Higgins (1970b) proposed a solution for the nondimensional cross-shore profile of the alongshore current as follows

(1a) $\quad$ V(X,P)= $\qquad$
$$V(X,P)= \begin{cases} B_1 X^{p1} + AX & 0 < X < 1 \\ \left(P(1-p2)(p1-p2)\right)^{-1} & X=1 \\ B_2 X^{p2} & 1 < X < \infty \end{cases}$$

(1b) $\qquad A = 1/\left(1 - \dfrac{5}{2}P\right); \; P \neq \dfrac{2}{5}$

(1c) $\qquad B_1 = \dfrac{(p2-1)}{(p1-p2)}A$

(1d) $\qquad B_2 = \dfrac{(p1-1)}{(p1-p2)}A$

(1e) $\qquad p1 = -\dfrac{3}{4} + \left(\dfrac{9}{16} + \dfrac{1}{P}\right)^{1/2}$

(1f) $\qquad p2 = -\dfrac{3}{4} - \left(\dfrac{9}{16} + \dfrac{1}{P}\right)^{1/2}$

P is a nondimensional parameter that represents the extent of horizontal mixing in the surf zone and under Longuet-Higgins' (1970b) formulation was estimated a function of beach slope and the drag coefficient. $X = x/x_b$ is the nondimensional cross-shore distance and $V = v/v_0$ is the nondimensional velocity. x is the cross-shore distance and x_b is the surf zone width defined as the distance offshore where wave breaking is initiated. v is the longshore current as a function of the offshore distance and v_0 is the peak longshore current if there were no horizontal mixing. The following equation is used when $P = 2/5$:

(2) $\quad$ V(X,2/5)=
$$V(X,2/5)= \begin{cases} \dfrac{10}{49}X - \dfrac{5}{7}X\ln X & 0 < X < 1 \\ 0.2041 & X = 1 \\ \dfrac{10}{49}X^{-5/2} & 1 < X < \infty \end{cases}$$

The total longshore component of the radiation stress as set forth by Longuet-Higgins can be determined by the offshore wave height and wave angle. Within the surf zone, wave energy dissipated by wave breaking forces the longshore current, thus the local radiation stress could be determined by the local wave height and wave angle. The local stress is what would drive the longshore current at any particular cross-shore location (Longuet-Higgins, 1970a). Subsequent modeling efforts utilized this idea to develop longshore current models that did local predictions using detailed bathymetric measurements. Longuet-Higgins (1970) did not do a localized determination of the radiation stress within the surf zone but instead assumed the beach was planar and the wave amplitude decay across the surfzone could be defined by the relationship $a = \gamma h$ (Munk 1949) where a is the wave amplitude, h the local water depth, and γ is the wave breaker criterion (assumed to be 0.3 to 0.6). When there is no horizontal mixing, equations (1) predict a saw tooth longshore current profile with the peak current at the break point and a monotonic decrease to zero at the shoreline (See figure 1). As mixing is introduced,

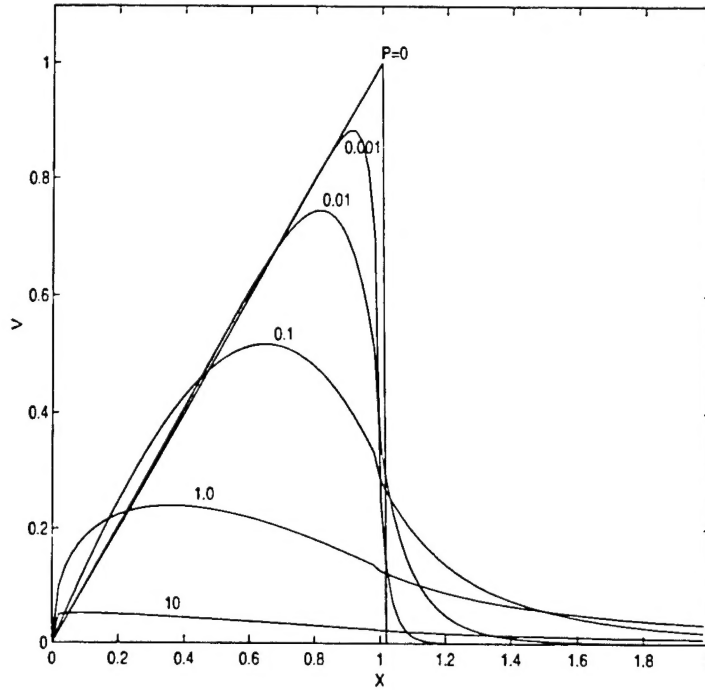the profile becomes smooth with the peak positioned shoreward.

Figure 1. Family of nondimensional longshore current profiles as P varies from 0 to 10.

The nondimensional position of the maximum can be determined by differentiating equation 1(a), setting the derivative equal to zero, and using equation (1c) to solve for X_{max} which can then be used in equation (1a) to calculate V_{max}. The results are shown in equations 3 below.

(3a)
$$V_{max}(P) = (1 - 1/p1) A X_{max}$$

(3b)
$$X_{max}(P) = \left(\frac{p1 - p2}{p1 \, (1 - p2)} \right)^{1/(p1 - 1)}$$

Komar (1979) presented an equation for the maximum longshore current in terms of the amount of energy supplied to the nearshore as a function of breaker wave height and direction:

(4)
$$\hat{v}_{max} = 1.17 \sqrt{g H_b} \sin \alpha_b \cos \alpha_b$$

where H_b is the measured wave breaker height, g is gravity, α_b is the measured breaker

angle relative to shore normal, and $\hat{v}_{max}$ is the predicted maximum longshore current. He used

measured longshore currents from near the mid surf and the concurrent breaker wave height

and angle to develop his model and made the assumption that the maximum current is near the

mid surf position. The data were a combination of laboratory and field measurements.

It is important to note that all of these relations (equations 1-4) were derived for planar

beaches and monochromatic waves. Analytical solutions of this form have only been applied to

experimental data where these assumptions have been justified. Also note that if the waves are

monochromatic and that wave breaking is depth dependent, idealized waves of a given height

all break at the same offshore location.

Later investigators used Longuet-Higgins (1970a) premise that if the local wave height

within the surf zone is known, then the local forcing for the longshore current can be

determined. This affords the opportunity to apply these models to more complex topographies.

Those that are relevant to Duck are described below. Thornton and Guza (1986) presented a

numerical model also based on alongshore momentum flux (radiation stress) but for arbitrary

bathymetry and random waves. In their model, the longshore current was forced by the

gradient in radiation stress which was balanced by the bottom shear and Reynold's stresses.

The radiation stress gradient is produced by the wave height transformations as a result of

wave breaking. Their model predicted wave height transformation across the surf zone and the

resultant cross-shore profile of the longshore current quite well for a planar beach with relatively

straight and parallel bottom contours (figure 2a). Thornton and Kim (1993) attempted to apply

that model to Duck in an analysis of tidal modulation of the longshore current. They used

measured bathymetric profiles and longshore currents from the DELILAH experiment. The
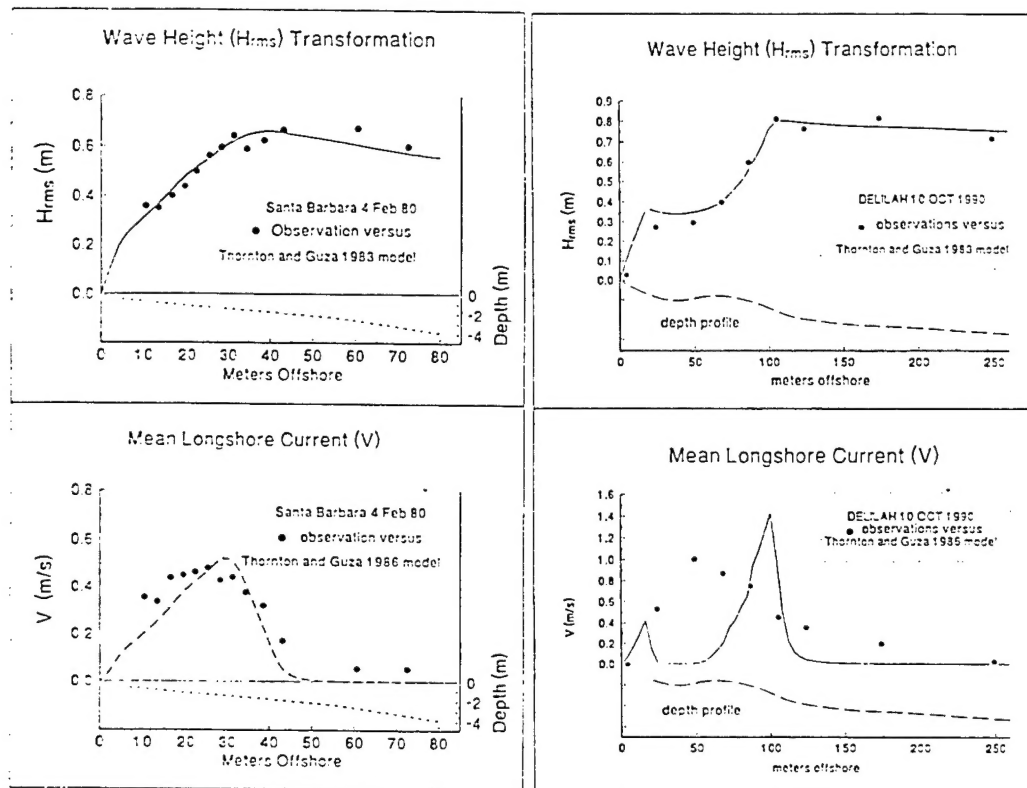

Figure 2. Wave height transformation and cross-shore profiles for a planar and barred beach

model correctly predicted the wave height transformation across the surf zone including the two

regions of wave breaking over the bar crest and on the beach face (figure 2b). The predicted

profiles of the longshore current showed a peak in the longshore current near the bar and

another smaller peak near the shoreline (the local maxima in the gradient of the momentum

flux) with a minimum in the trough and were largely dissimilar to observations which had a

single peak in the region of the trough. Smith et al (1993) used a similar wave transformation

and longshore current model (Kraus and Larson, 1991 and Larson and Kraus, 1991). They

tested their model using eight profiles from the DELILAH experiment. Their model predicted two

peaks in the longshore current profile (similar to Thornton and Kim, 1993) which resulted in an

average least squares error of 55.9% when compared to the measured longshore currents but the average least squares error for the wave height transformation across the surf zone was only 8.0%. In an attempt to explain the current profile mismatch, Reiners et al (1995) investigated the influence of longshore pressure gradients at Duck during the DELILAH experiment (figure 3). They proposed that the current profile peak over the trough may have been the result of variations in wave set-up due to small topographic variations in the alongshore direction that resulted in a stronger than expected current over the trough [theorized by Symonds and Huntley (1980)].   Their predictions still showed a single peak over the
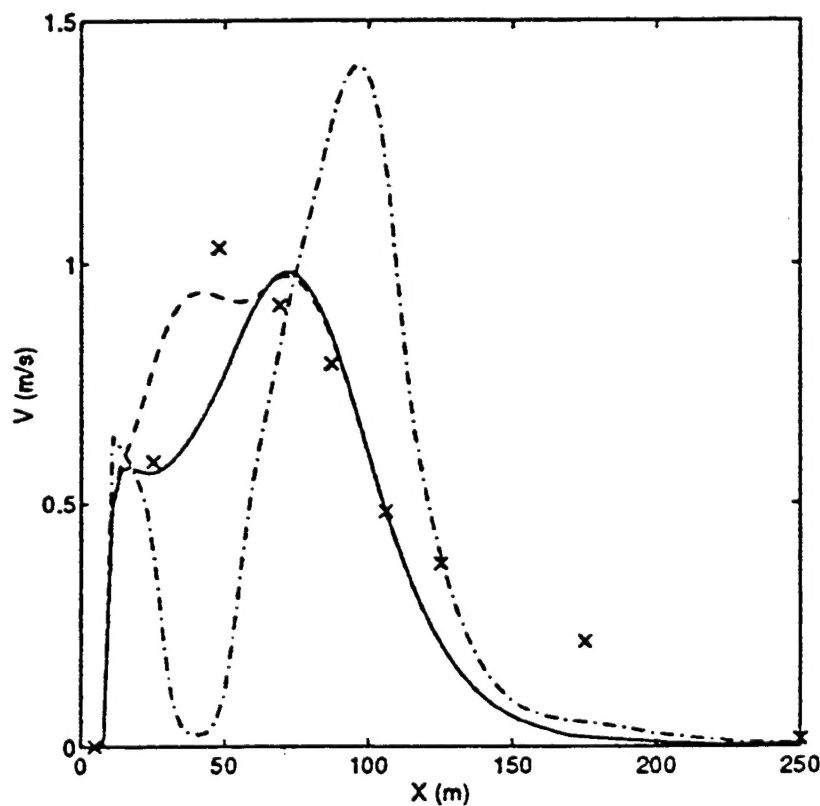

Figure 3. Predicted longshore currents compared with measured currents. The dashed line is the prediction including pressure gradient, rollers and mixing, the solid line is without the pressure gradient term, the dash-dotted line is the predicted current with no pressure gradient, roller or mixing, and observations are x marks. (from Reiners et al 1995)

shoreward portion of the bar crest with a broad region over the trough where the longshore current was larger than earlier predictions. The longshore current then diminished to zero at the shoreline. While their model is an improvement, the observed peak was in the trough region approximately 30 m shoreward of the predicted peak.

These prior studies indicate that many of the longshore current models that incorporate the details of wave height transformation across the surf zone, wave momentum thrust across the surf zone, and detailed knowledge of the bathymetry often do not adequately reproduce even the general shape of the measured cross-shore profile of the longshore current. In fact, it is not unusual for the measured longshore current profile shape from a complex topography to resemble profiles from beaches that have a simple topography (Allender et al, 1978; Komar and Oltman-Shay, 1990; Smith et al 1993; Thornton and Kim, 1993) (see figure 2). The DELILAH experiment indicates that the cross-shore profile was qualitatively similar to that expected for a planar beach with the maximum longshore current found in the trough (which is near the mid surf region if the surfzone is considered to be from the bar crest to the shoreline). The bottom line is that these detailed models predict the wave height transformation across the surf zone quite well, but the corresponding distribution of the longshore current is not well predicted. The processes involved which distribute the energy in the longshore current are, at this time, not well understood.

Given these results, it may be advantageous to utilize the total momentum thrust available to force the longshore current rather than a more detailed approach involving localized effects to develop an operational model of the longshore current. Longuet-Higgins (1970b) makes the point that if the offshore wave height and wave angle are known then the total alongshore component of the wave momentum is known. The concept of horizontal mixing can then be used to distribute the longshore current across the surf zone. This does not require detailed measurements of radiation stress gradients (or bathymetry) within the surf zone. In addition, by

using a relation similar to equation 4, the maximum current can be estimated by using these same offshore measurements of wave height and angle. The resulting nondimensional profile is then scaled by the estimate of the maximum current and the surf zone width. The real advantage is that only the total alongshore component of radiation stress is required which can be determined by the wave height and angle offshore of the surf zone. The model would be applied for all beach profiles even when the assumption of a planar beach is clearly violated.

Objective

The basic goal of this work is to develop a longshore current model that will give an adequate representation of the current profile through the surf zone and not require detailed inputs to do so. The application of the model is geared toward naval forces which typically conduct operations in data restricted regions. Thus, ideally, these model inputs could be limited to only visual observations of the wave height, wave angle, and the surf zone width. We use a method similar to that summarized by Komar and Oltman-Shay (1990) where equation 1 is used to estimate the cross-shore profile shape. An equation analogous to equation 4 is used to estimate the peak current for the current profile as a function of wave height and wave angle. These are combined in this model into a single relationship that predicts the cross-shore profile of the longshore current Longuet-Higgins (1970b) suggested that P is a function of beach slope and drag coefficient. Since the objective of this work is a model that uses readily observable inputs, we set P to a constant value. As will be seen, this did not significantly affect the quality of the predictions.

MODEL DEVELOPMENT

Experimental Description

The data to develop the model were from DELILAH (Duck Experiment on Low-frequency and Incident-band Longshore and Across-shore Hydrodynamics) which was conducted 2-20 October 1990 at the US Army Corps of Engineers Field Research Facility (FRF) located at Duck, North Carolina. The FRF is located on the Atlantic side of a barrier island whose beach is typically barred. The objective of DELILAH was to measure the three dimensional response of the bathymetry to wind and wave forcing. Longshore current variations due to tidal variation were also examined. For further details see Birkemeier (1991).

The primary station deployment (figure 4) was a dense cross-shore array of nine stations labeled 10, 20,... 90 located north of the pier (Birkemeier 1991). Station 10 was deployed near the shoreline and was intermittently exposed during low tide. Station 90 was deployed

approximately 250 m offshore at a depth of 4 m. Stations were most closely spaced in the
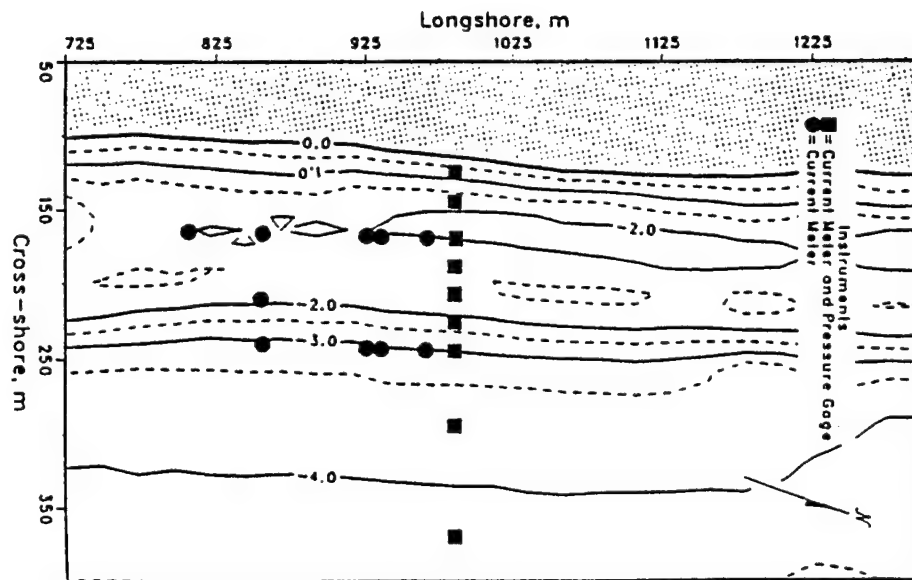

Figure 4. Instrumentation placement during DELILAH. Bathymetry is from 12 October
(from Church and Thornton, 1993)

vicinity of the offshore bar. Each station consisted of a collocated pressure sensor and a Marsh-

McBirney electromagnetic current meter mounted on a pipe which was jetted into the bottom.

Two shore parallel arrays of electromagnetic current meters were deployed at 50 m and 125 m

offshore. The array at 50 m was in line with station 30 of the shore normal array, consisted of

five electromagnetic current meters (stations 31-35), and was typically located in the trough.

The array at 125 meters was in line with station 70, had four electromagnetic current meters,

and typically was located on the seaward flank of the bar. Data were sampled at 8 hz and

statistics computed for 4096 data point (approximately 8 minutes) ensembles. The FRF also operates an array of 16 pressure gauges at the 8 m depth contour from which wave height and directional spectra are calculated every three hours (Pawka 1983). Also at the 8 m contour was a collocated pressure sensor and electromagnetic current meter (station 3511) from which an hourly wave direction was calculated using a method described by Oltman-Shay and Guza (1984). Since this station provided the most dense data coverage, it was chosen as the preferred station. This gave a total of 384 measurements of the cross-shore velocity profile of the longshore current, wave angle and wave height. Comparison with the linear array showed a moderate correlation (r=0.76) (figure 6) which indicates that 3511 gives as reasonable an estimate of the offshore wave angle as does that from the linear array. Wave angles from station 3511 were refracted to a depth of 3m using Snell's Law to provide estimates of the wave angles at the breakpoint. The wave height measured from station 70 located near the seaward base of the longshore bar is used as an estimate for H_b .

The experimental conditions varied significantly during DELILAH. Wave heights varied from less than 0.5 m to nearly 2 m and the longshore currents ranged from less than 0.1 m/s to greater than 1.5 m/s. The wind and wave forcing was primarily from the southeastern quadrant which resulted in northward flowing longshore currents throughout much of the experiment.
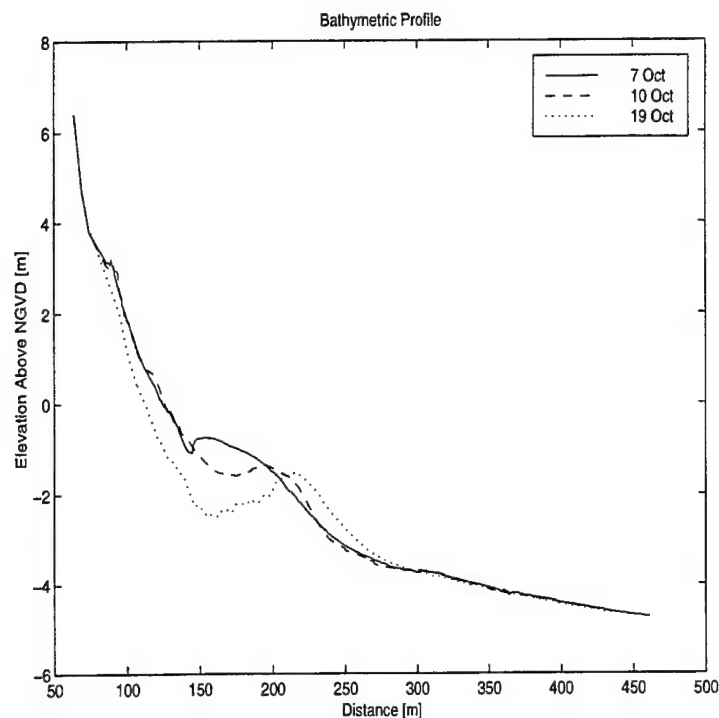
Bathymetric Profile

Figure 5. Typical bathymetric profiles depicting the changes
in the topography near the cross-shore sensor array.

Figure 5 shows three of the daily bathymetric profiles during DELILAH. The bar was present on

2 October approximately 60 m offshore when the experiment began. During the mild wave

conditions of 2-7 October, it migrated shoreward and welded to the beach. High waves

associated with a frontal passage on 10 October and swell waves associated with hurricane Lili

on 13 October resulted in the bar reforming approximately 100 - 110 m offshore near station 50

and remained at that location until the experiment's conclusion on 20 October (Thornton and
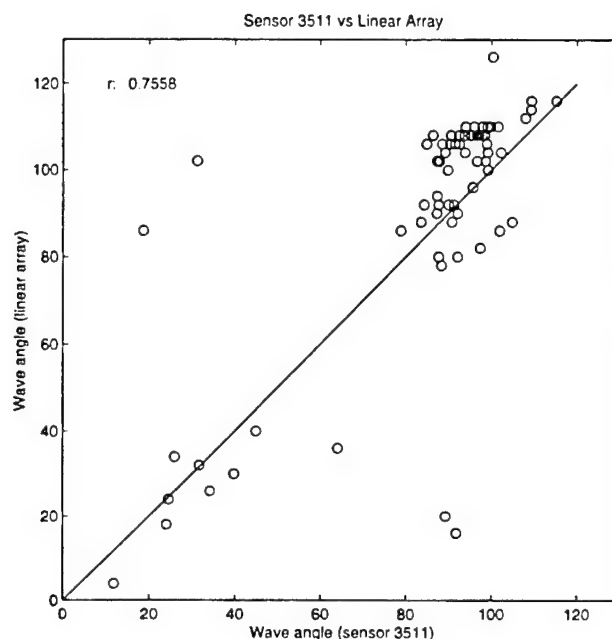
Kim, 1993).

Figure 6. A comparison of the two wave angle measurements at 8
meters. The angles are measured from magnetic North.

Daily visual observations of x_b (surf zone width) were available as well as video

observations which when combined provided 30 surf width observations during the period of 6-

16 October, 1990. The time of these observations, however, did not correspond exactly to the

times at which the cross-shore profiles of the longshore current were measured. Accordingly,

an estimator of the surf width for this experiment was used ($\hat{x}_b = mH_s$) where $m \approx 95$ was

determined by a linear fit of the surf width observations to the concurrent significant wave

height (H_s) measured at the 8 meter array. The linear fit was constrained to pass through the

origin. The results of the fit (figure 7) were then used to estimate the surf zone width at the time

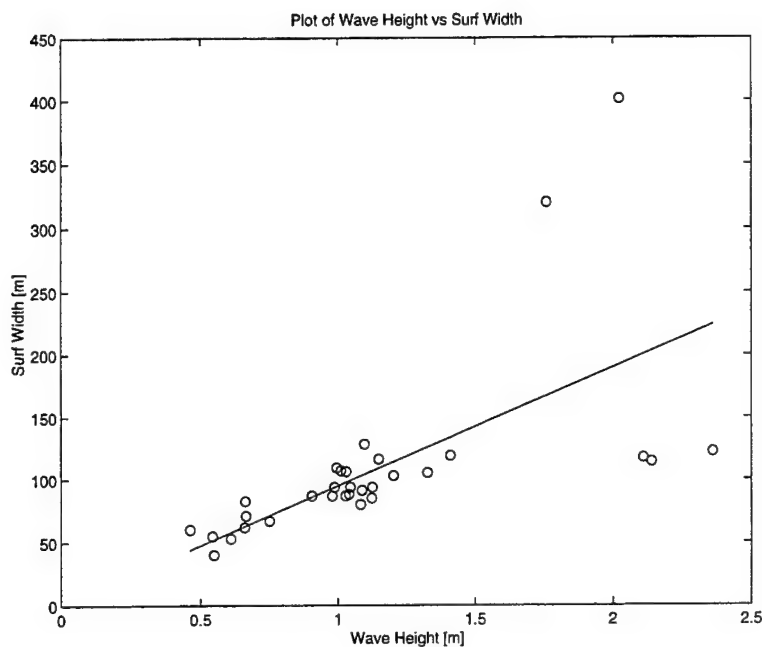of each cross-shore profile using the concurrent measured H_s.

Figure 7. Plot of the measured wave height and the observed surf zone width.

The estimated surf zone width $(\hat{x}_b)$ is fundamental to the model development, therefore, it is important to have some verification that the linear relationship given above is reasonable. One way of doing so is described as follows. Equation (5) is the relationship between wave height and the depth of initial wave breaking.

(5) $H_s = \gamma h_b$

Geometry shows that

(6) $\tan(\beta) = h_b / x_b$

From equations (5) and (6), one can derive

(7) $\dfrac{x_b}{H_s} = \dfrac{1}{\gamma \tan \beta}$

where γ is the breaker criterion for initiation of wave breaking, H_s is the significant wave height measured at the 8 m array and h_b is the depth at breaking, β is the mean slope, and x_b is the surf width. A visual examination of figure 5 shows that the depth of closure is approximately 3.5 m at an offshore distance of approximately 300 m. The mean position of the shoreline throughout the experiment was around 115 m. From this, a mean slope β of the beach from depth of closure to the shoreline is approximately 0.02. For the Duck data, the left hand side of equation 7 is the slope of the line (figure 7) which when used with an estimated β of 0.02 gives a γ of 0.52. This is within the range of values for Duck, NC (0.4 - 0.8) reported by Sallenger and Holman (1985) which implies that the data in figure 7 provides a reasonable relationship for this site from which $\hat{x}_b$ can be estimated from the measured H_s.

The surf zone width used here is essentially the observed value at the time of the predicted longshore current. The appendix gives a simple approach to estimate the surf zone width using limited bathymetric data and nearshore wave fields that may be forcasted several hours or days in the future.
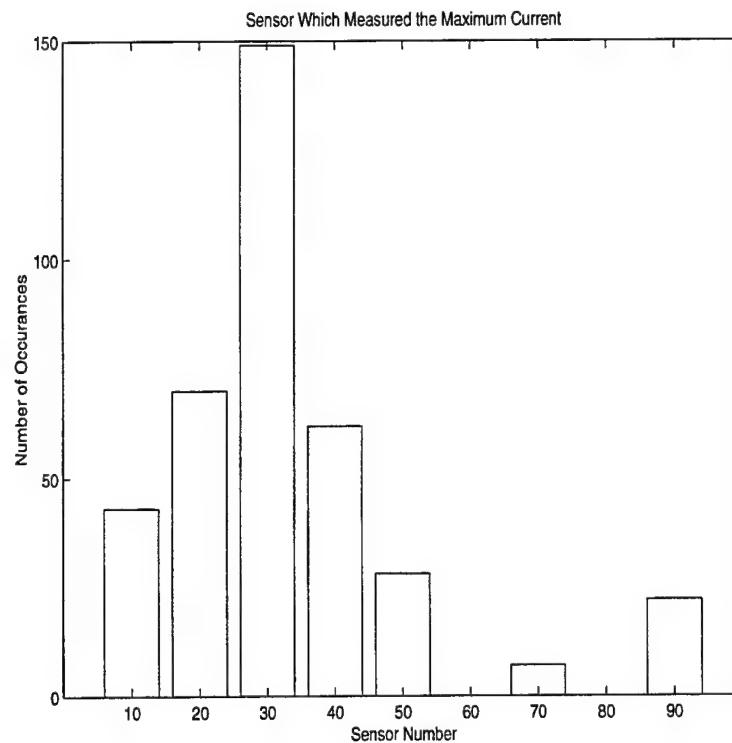
Sensor Which Measured the Maximum Current

Figure 8. Histogram of which stations measured the maximum current

Cross-Shore Profile Prediction

In order to have an adequate spatial sampling of the longshore current profile, profiles were selected where at least eight of the nine stations were operating for that particular time. In addition, profiles that had strange shapes that could not be modeled by any theory based on radiation stress (i.e. where the current maximum was on the beach face or outside the surf zone) were eliminated (figure 8). Profiles that had a peak current less than 0.2 m/s were also filtered out because they lacked significant structure. Longuet-Higgins' formulation does not allow for flow reversals in the cross-shore profile, so limited number of data runs having currents of opposite sign were also eliminated. These criteria generally matched the period of 6-

14 October and resulted in 118 usable longshore current profiles.

The first step in the model development was to determine a normalized representation of the typical shape of the cross-shore profile of the alongshore current during DELILAH. We chose to assume that bathymetry had no influence on the currents and that the profile shape was given by equations 1 - 3. We then solved for the best fit nondimensional profiles V for each run as function of P and X using the observed profile data. The cross-shore velocity measurements were non-dimensionalized using v_{max} (the measured maximum current) and $\hat{x}_b$.

P was determined using an iterative algorithm to minimize the error between the measured longshore current profiles and profiles predicted using equations 1 and 2. It is based on a golden section search and a parabolic interpolation which is described in detail by Forsythe et al (1976). The algorithm searched for the best fit of P between 0.005 to 2. Measured inputs were x_{obs} (cross-shore location of the current meters), v_{obs} (the current measurements at those locations), v_{max} (the observed maximum within v_{obs}), and $\hat{x}_b$.

The resultant distribution of P values for the DELILAH data is given in figure 9. The mode is around 0.15 and the mean is 0.58. Longuet-Higgins (1970b) compared his theoretical development with the laboratory data of Galvin and Eagleson (1965) and found that P was generally 0.01 to 0.4 (Longuet-Higgins, 1970b) with a mode of 0.15. Therefore, the values from the DELILAH data have wider range than those from the data of Galvin and Eagleson (1965) but have similar modal values. The large peak in figure 9 at 2 is due to convergence difficulties in the error minimization algorithm for those cases where the curve of P vs error is nearly flat.
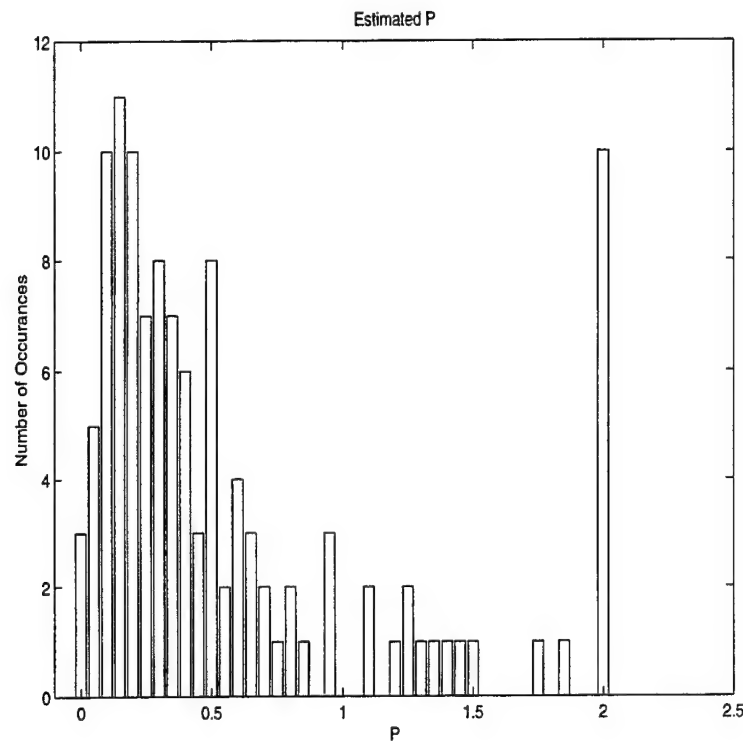
Figure 9. Histogram of the best fit P for each measured longshore current profile.

Longuet-Higgins (1970b) noted that the cross-shore profile shape is not particularly sensitive to P (in comparison with the influence of x_b and v_{max}). For example, varying the mixing parameter P from 0.001 to 1.0 (three orders of magnitude) results in a nondimensional velocity maximum, V_{max} that varies from 0.88 to 0.24, a factor of four (figure 1). With this in mind, the operational use of this model would be greatly simplified if a single P value could be used which would give reasonably good results. Accordingly, a value for P was selected such that it gave an over all minimum normalized error when used for all the measured cross-shore profiles. The procedure and results of this analysis are given below.

P was varied from 0.005 to approximately 2 in increments of 0.01. For each value of P

within this range, a profile was generated for comparison to measured profiles. A normalized error was computed for each profile using the measured data.

$$(8a) \qquad err_j = \frac{1}{NO} \sum_{i=1}^{NO} |\hat{v}_i - v_{obs,i}| / v_{max,j}$$

where NO is the number of measurements in profile j; $\hat{v}_i$ and $v_{obs,i}$ are the respective estimated and measured longshore currents at the cross-shore location i of profile j; and $v_{max,j}$ is the measured maximum in the longshore current. A mean normalized error for all the profiles over which P was calculated was defined as

$$(8b) \qquad \bar{e} = \frac{1}{NP} \sum_{j=1}^{NP} err_j$$

where NP is the number of profiles. P was incrementally increased to the next value and the above process repeated. The results of this analysis are plotted in figure 10. The value of P that gave the minimum for all measured profiles (denoted as P_{min}) was 0.37 with a mean normalized error, $\bar{e}$, of around 17%. In contrast, the mean normalized error for all profiles using the P derived from the minimization algorithm for each profile is 15%. So, the adverse impact of selecting a single P for all profiles was not significant.
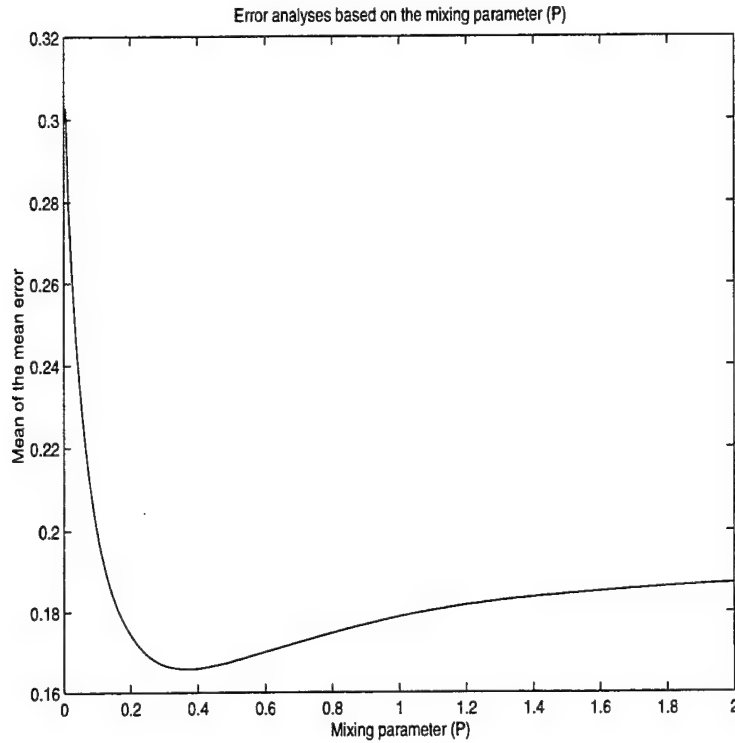
Figure 10. Plot of the mixing parameter P vs the mean normalized error for all
profiles.

Maximum Current Prediction

In the above formulation, model predictions were dimensionalized using the measured maximum current. Since no such measurement is typically available in an operational scenario, a prediction of the maximum current is required. Equation 9 is used to estimate the maximum longshore current which in turn is used to scale the nondimensional velocity from equations 1-3.

(9) $v_{max}(H_b, \alpha_b) = C\sqrt{gH_b}\sin\alpha_b\cos\alpha_b$

where $v_{max}(H_b, \alpha_b)$ is the measured current maximum and C is a coefficient determined by

linear least squares fit of equation 9 to the measured data.

Figure 8 clearly shows that stations 10 through 50 accounted for the great majority of the measured maximum current. Accordingly, the profiles were screened to select those profiles where the maximum was measured by one of those stations. Although all the stations did not need to be working we did require that the trough stations (20 - 40) were operational since the peak current was typically in the trough. This screening resulted in 254 data points.
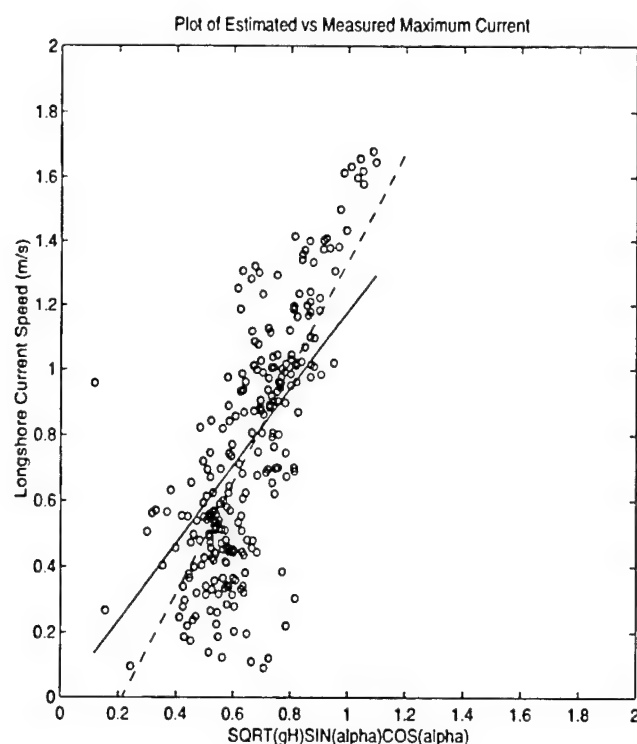

Figure 11. Plot of the estimated maximum longshore current vs the measured maximum longshore current. The solid line is a linear least squares fit to the data that is constrained to pass through the origin. The dashed line is not so constrained.

A least squares fit of the measured maximum currents and that predicted by equation 9 was done. In principal, if there was no alongshore wave forcing then there can be no wave induced longshore current and the y-intercept of a linear fit of equation 9 to the data would be

zero. Therefore, we chose to require the fit to pass through the origin. Additionally, one would expect that a fit constrained to pass through the origin could be more generally applied to other beaches. The results are shown in figure 11. The slope of the best fit line was 1.18 ± 0.05. The correlation coefficient was 0.48 and was statistically significant at the 95% confidence level and accounted for 28% of the observed variance. The slope of this line was quite close to that obtained by Komar (1979) for a planar beach ($C = 1.17$). This indicates that as a minimum, the prediction for the maximum longshore current can be generally applied for either a planar beach or more complex bathymetry. However, we should mention that the skill of the model increased if a y-intercept was allowed. Therefore, a fit of the data was done that was not constrained to pass through the origin. This result is depicted as the dashed line in figure (11). The slope was 1.70 and the y-intercept was -0.36. The correlation coefficient was 0.75 which was statistically significant at the 95% confidence level and explained 57% of the observed variance in the data. Possible mechanisms that could cause the linear fit of the data to not pass through the origin include wind forcing and pressure gradients caused by alongshore variations in wave set-up. An examination of the wind revealed that 65% of the time the wind direction was from the ESE clockwise through the WSW (the southern semi-circle) which would have enhanced the northward flowing wave generated longshore current. Reiners et al (1995) showed that alongshore pressure gradients may have been a factor during DELILAH. Their results also indicated that these gradients would enhance the longshore current in the trough region. Both of these mechanisms would produce longshore currents greater than expected based only on wave forcing which would have resulted in a positive value for the y-intercept. An examination of figure (11) indicates an opposite trend in the data with a y-intercept of -0.36. Since there is no adequate explanation for a process that could cause the apparent offset, we chose to use the fit that passed through the origin.

SEMI-EMPIRICAL LONGSHORE CURRENT MODEL

The final model of the cross-shore profile of the longshore current was derived from the two component models. The first is a means to predict the nondimensional cross-shore profile of the longshore current from equation 1 using $P_{min} = 0.37$. The second is to predict the maximum current which is given by equation 9 where $C = 1.18$. Using these two components, equations 1 can be reduced to

$$(10) \quad \hat{v}(x, x_b, H_b, \alpha_b) = \begin{cases} \left(-32.30 \left(\dfrac{x}{x_b} \right)^{1.057} + 43.78 \left(\dfrac{x}{x_b} \right) \right) \left(\sqrt{gH_b} \sin\alpha_b \cos\alpha_b \right) & 0 < \dfrac{x}{x_b} \leq 1 \\[2em] \left(0.69 \left(\dfrac{x}{x_b} \right)^{-2.557} \right) \left(\sqrt{gH_b} \sin\alpha_b \cos\alpha_b \right) & 1 < \dfrac{x}{x_b} < \infty \end{cases}$$

where x is offshore distance, x_b is the observed surf zone width, H_b is the observed breaker height, and α_b is the observed breaker angle. Note that in the dimensionalization $\hat{v}_{max} / \hat{V}_{max}$ was incorporated into equation 10 using $\hat{V}_{max} = 0.36$ from equation 3 where $P_{min} = 0.37$.

MODEL APPLICATION

The combined model was tested with the DELILAH data to predict the cross-shore profile

of the longshore current using equation (10). Example runs are shown in figures 12 a-d.
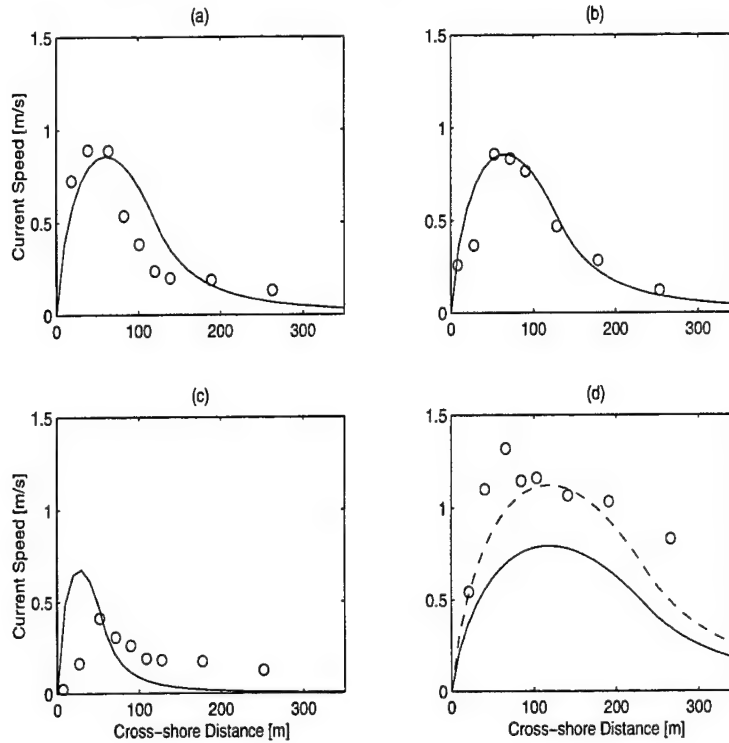

Figure 12. Plots of the predicted cross-shore profile of the longshore current vs the measured profiles. Panel (a) is from 1200 October. Panel (b) is from 2100 11 October. Panel (c) is from 0500 7 October. Panel (d) is from 2300 12 October. Circles are measured data and solid lines are the predicted profiles.

The estimated surf width ($\hat{x}_b$) was utilized in the model application. Using an error statistic calculated with equation (8) where the predicted maximum longshore current ($\hat{v}_{max}$) is used in the place of the observed maximum (v_{max}), the average absolute deviation for all profiles was 19% with a minimum of 9% and maximum of 51%. Figure (12a) shows a typical fit where the observed model error is near the mean value of 19%. The match between the predicted and the measured maximum current was quite good, the predicted maximum current is within 0.10 m/s of that indicated by the measured currents, although the predicted maximum is slightly seaward of that measured. Figure (12b) shows an example of an exceptionally good fit between the estimated and measured peak current (9% error). Figure (12c) is an example of

when the model did not predict as well (30% error). There is a relatively large difference in both the magnitude and location of the current peak. Given that the measured currents were small (less than 0.5 m/s) the errors in the predictions may be related to a highly variable breaker angle, α_b, often observed under low energy conditions. Also, with reference to figure (11), the fit that passes through the origin typically over predicts the maximum longshore current when the measured values are low, which can be seen in figure (12c). Figure (12d) is an example of when the model prediction was particularly bad, the error being 51%. At this time there were large waves associated with hurricane Lili. These large waves resulted in an exceptionally wide surf zone that encompassed station 70 which provided estimates of the breaker height. If the breaker wave heights were actually greater, the peak current would have been under estimated. The dashed line in figure (12d) is a prediction of the longshore current profile if the breaker height were twice the wave height measured by station 70. A visual comparison shows a much better agreement with the observed measurements.

Figure 13 is a histogram of the average percent error for all of the profiles. From this it is clear that in the most cases, the error is between 10% and 30% and errors greater than 30% relatively rare. These accuracies are greatly improved over previously published model results
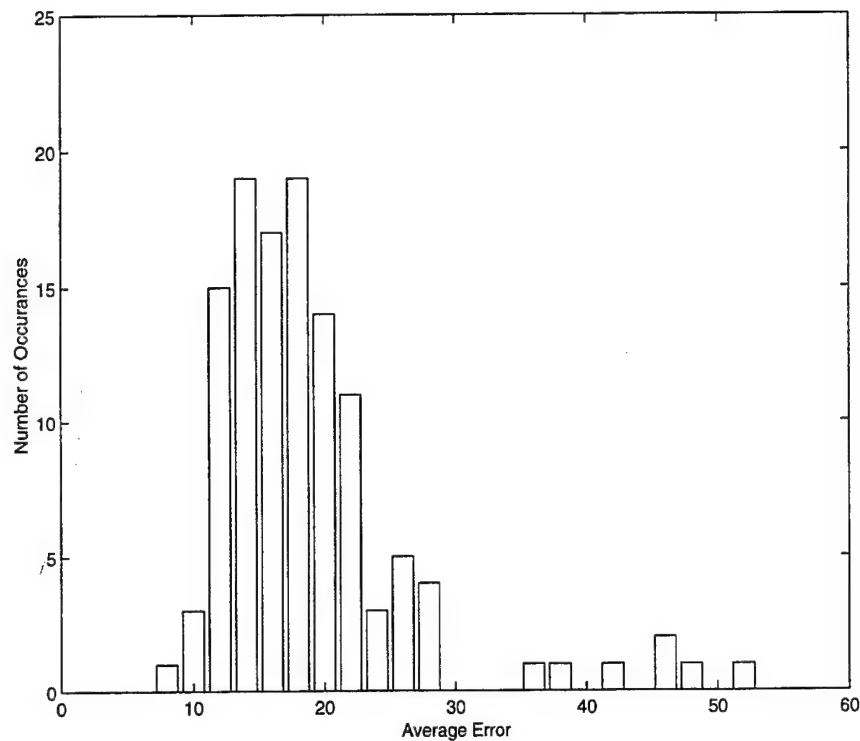
for the same data.

Figure 13. Histogram of the average error for all profiles.

In an operational scenario, an important aspect of longshore current modeling is the magnitude and cross-shore location of the longshore current. Figures 14 and 15 show the comparison between the measured longshore current maximum and the predicted maximum. Before the comparison was made, a cubic spline interpolation (de Boor, 1978) of the measurements was done to more precisely determine the location and magnitude of the longshore current maximum. Figure 14(a) is the distribution of the absolute difference between the measured and predicted magnitude of the longshore current. The average difference was approximately 0.20 m/s with maximum of 0.55 m/s and the minimum difference was less than

0.05 m/s. Figure 14(b) shows that the percent difference ranged from near zero to 100% while
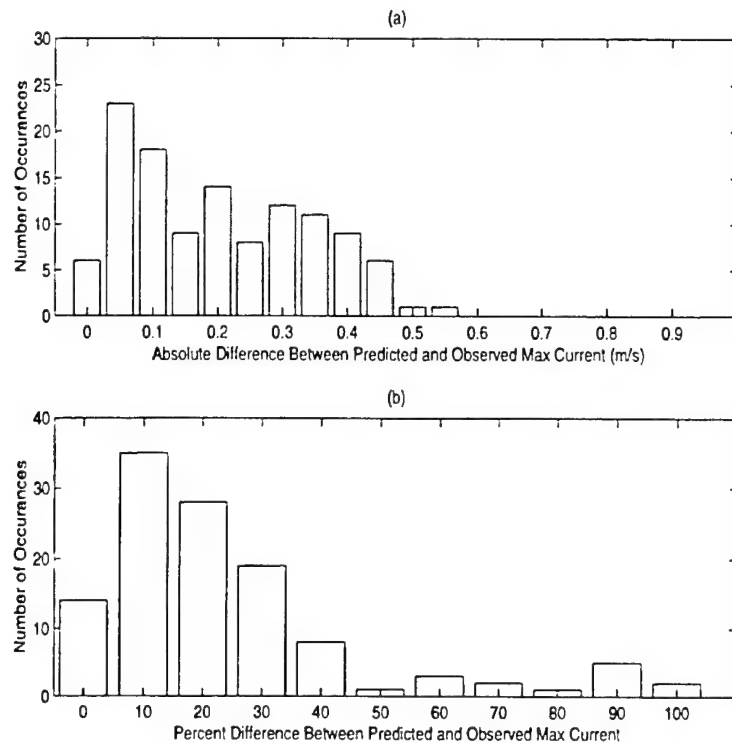

Figure 14. Distributions of the difference between predicted and measured maximum current.

the majority of the cases the difference was less than 30% difference. The average difference was 25%. Figure 15(a) shows the distribution of the absolute difference in the cross-shore location of the longshore current maximum. The average difference was 20 meters and ranged from zero to 60 meters. The differences were also normalized by the surf zone width (figure

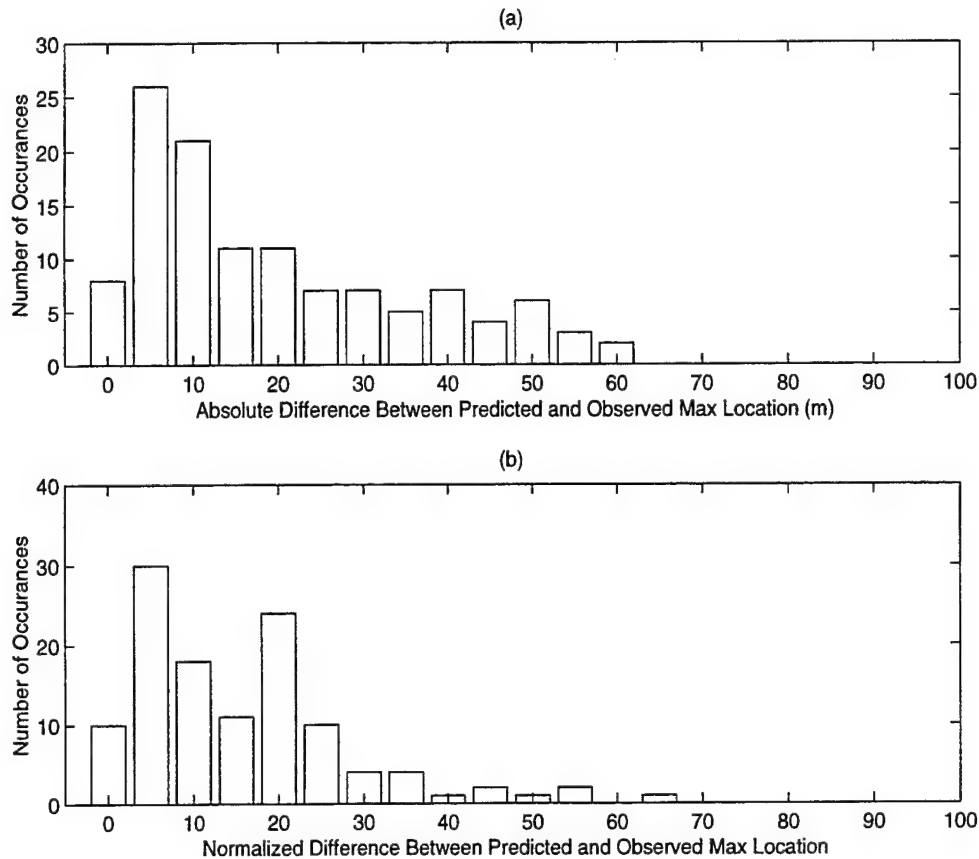15(b)). The normalized difference was 16% of the surf zone width.

Figure 15. Distributions of the difference between the predicted and observed maximum current cross-shore location.

A linear regression of the average error for each profile versus the individual model inputs for each profile was done to determine the model sensitivity to these inputs. The results are summarized in Table I. The correlation coefficients (r) between the average error for each profile and the model inputs are low ranging from 0.25 to 0.5 but were significantly greater than zero at the 95% confidence level. However, the regression accounted for at most 25% of the variation about the mean and generally was 10% or less. Based on this result, the model appears to be fairly robust for the data set from which it was developed. Better insight to the model sensitivity will be gained when it is applied to other data sets from Duck and other locations.

Table 1:

	α_b	H_b	X_b	$\hat{v}_{max}$
r	0.51	0.32	0.31	0.25
% Variance	25.6	10.0	9.3	6.1
Significant	Yes	Yes	Yes	Yes

DISCUSSION

A semi-empirical model of the longshore current has been developed that is simple and reasonably accurate for operational applications, particularly in regions where field measurements are limited or unobtainable. This model was derived using the simple theory developed by Longuet-Higgins (1970a,b) and practical insights gained from subsequent field experiments. The only inputs required are the observed wave breaker height, wave breaker angle and the surf zone width. The model does not require knowledge of the bathymetric profile and can be applied to both barred and planar beaches. In spite of its simplified nature, this semi-empirical model has produced an operationally useful prediction of the longshore current profile.

The observed inputs can be obtained by several methods and lend themselves well to information that can be directly gleaned from visual observations, video imaging and/or photographic reconnaissance, or the output of other models that may be more regional/global in character. Of particular note is the emerging use of off-the-shelf video technology for nearshore and coastal studies (e.g. Holland et al, 1997). Not only can it provide all the inputs to this model, but other measurements can be derived that have direct application in other

aspects of the operational use by the Navy.

The constant for the current maximum prediction (equation 9) is quite similar to that presented by Komar (1979), although Komar derived his from laboratory data and limited field data all of which were from planar beaches. This implies that at least this aspect of the model can be generally applied to any beach. Additionally, field observations indicate that the shape of the longshore current profile is similar for both a planar beach and a barred beach. The value of P_{min} puts the longshore current peak in the mid surf location which is consistent with a number of observations of the longshore current summarized in Komar and Oltman-Shay (1990).

The utility of this model is that it uses the total alongshore wave momentum flux entering the surf zone and distributes it using an empirical horizontal mixing parameter that produces a longshore current profile that is consistent with observations from Duck (figures 12-15). This approach is in contrast to the more detailed model developed by Thornton and Guza (1986) and that which was employed by Smith et al (1993). Both these models predicted a more complex structure to the longshore current profile than observed (figure 2). This is a clear indication that another process (or processes) are involved that distribute the longshore current energy. As described earlier, Reiners et al (1995) proposed that alongshore pressure gradients may be responsible for the disparity between predictions and observations at Duck. While they demonstrated an improvement, it did not match the observed cross-shore profile of the longshore current. Their approach requires a detailed three-dimensional bathymetry. Such detail will not be available in an operational setting and is difficult to obtain in a research setting.

Shear instabilities in the longshore current is one horizontal mixing mechanism that shows promise. Church (1993) analyzed the DELILAH data and found that mixing produced by shear instabilities was qualitatively sufficient to bring the more detailed longshore current models into agreement with observations on a barred beach. This opens the possibility of estimating the

strength of mixing due to shear instability by the predicted magnitude of the longshore current. If such a relationship can be verified, then there is the potential to estimate the horizontal mixing as a function of the input wave momentum flux to the surf zone rather than depending on a fixed mixing parameter as does the present model.

The Navy does employ the Navy Standard Surf Model (NSSM) to support its operations in coastal regions (Earle, 1989). The basis of that model is the approach used by Thornton and Guza (1986). Until recently, the NSSM has not been thoroughly tested against measured data (Hsu et al, 1997). The data used in the test were from DELILAH. The results show that the NSSM predicts the wave height transformation across the surf zone quite well, but the longshore current predictions do not compare favorably with the observations. In short, the NSSM exhibits the same strengths and weaknesses of the more detailed models from which it was derived.

There is no obvious restriction of this semi-empirical model that would preclude general application to other beaches. This applicability, however, has not been demonstrated and a more complete testing of the model validity is required. There are a few high quality data sets available and such testing will be done. The model can be tested in operational settings as well to test its utility for operational units of the Navy.

SUMMARY

A semi-empirical longshore current model has been developed that is not reliant upon bathymetry. The model inputs are wave breaker height, wave breaker angle, and the surf width. The output is a cross-shore profile of the longshore current that is consistent with field observations for both planar and barred beaches. The model was developed and tested from data gathered at Duck, NC during the DELILAH experiment in October, 1990. The average

absolute deviation of the model compared to the measured data was 19%. The beach at Duck had an offshore bar during the data collection. The model will require further testing to verify its general application for both plane and barred beaches.

REFERENCES

Allender, J.H. and J.D. Ditmars, Field measirements of longshore currents on a barred beach, Coastal Engineering, 5, 295-309, 1981.

Birkemeier, W.A., Samson and Delilah at the FRF, The CERCular, CERC-91-1, 1-6, 1991.

Church, J.C. and E.B. Thornton, Effects of breaking wave induced turbulence within a longshore current model, Coastal Engineering, 20, 1-28, 1993.

Church, J.C., Topics in longshore currents, PhD Dissertation, Naval Postgraduate School, 124p, 1993.

de Boor, C., A Practical Guide to Splines, Springer-Verlag, 1978.

Earle, M.D., Navy Surf Forecast Software: Scientific Reference Manual, NORDA Tech. Rep. 351, 180p, 1989.

Forsythe, G.E., M.A. Malcolm, and C.B. Moler, Computer Methods for Mathematical Computations, Prentice-Hall, 1976.

Galvin, C.J. and P.S. Eagleson, Experimental study of longshore currents on a plane beach, U.S. Army Coast. Eng. Res. Center, Tech. Mem. 10, 1080, 1965.

Holland, K.T., R.A. Holman, T.C. Lippman, J. Stanley, and N. Plant, Practical use of video imagery in nearshore oceanographic field studies, Jour. of Oceanic Engineering, 20 (1) 81-92,

1997.

Hsu, Y.H.L., T. Mettlach, E. Kennely, and M.D. Earle, Interim report on the validation of the Navy Standard Surf Model, NRL Memorandum. Rep. (submitted), 1997.

Komar, P. D., Beach-slope dependence on longshore currents, Journal of Waterway, Port, Coastal, and Ocean Engineering, 105, 460-64, 1979.

Komar, P.D. and J. Oltman-Shay, Nearshore currents, in Handbook of Coastal and Ocean Engineering, Vol 2, edited by J.B. Herbich, 651-680, Gulf Publishing Co., Houston, 1990.

Kraus, N.C. and M. Larson, NMLONG: Numerical model for simulating the longshore current, Tech Rep. DRP-91-1, 166p, U.S. Army Eng. Waterw. Exp. Stn. Vicksburg, MS, 1991.

Larson, M. and N.C. Kraus, Numerical model of longshore current over bar and trough beaches, J. Waterw. Port Coastal Eng., v 117 n 4, 326-347, 1991.

Longuet-Higgins, M.S. and R.W. Stewart, Changes in the form of short gravity waves on long waves and tidal currents, Journal of Fluid Mechanics, 8, 565-583, 1960.

Longuet-Higgins, M.S. and R.W. Stewart, the changes in amplitude of short gravity waves on steady non-uniform currents, Journal of Fluid Mechanics, 10, 529-549, 1961.

Longuet-Higgins, M.S. and R.W. Stewart, Radiations stress and mass transport in gravity waves, with application to surf beats, Journal of Fluid Mechanics, 13, 481-504, 1962. .

Longuet-Higgins, M.S. and R.W. Stewart, A note on wave set-up, Journal of Marine Research, 21, 4-10, 1963.

Longuet-Higgins, M.S. and R.W. Stewart, Radiation stresses in water waves; a physical discussion, with applications, Deep-Sea Research, 11 (4), 529-562, 1964.

Longuet-Higgins, M.S., Longshore currents generated by obliquely incident sea waves, 1, J. Geophys. Res., v 75, 6778-6789, 1970a.

Longuet-Higgins, M.S., Longshore currents generated by obliquely incident sea waves, 2, J. Geophys. Res., v 75, 6790-6801, 1970b.

Munk, W.H., The solitary wave and its application to surf problems, Ann. N.Y. Acad. Sci. 51, 376-424, 1949.

Pawka, S.S., Island shadows in wave directional spectra, J. Geophys. Res. 88(C4), 2579-2591, 1983.

Oltman-Shay, J.M. and R.T. Guza, A data-adaptive ocean wave directional-spectrum estimator for pitch and roll type measurements, Journal of Physical Oceanography, 14 (11), 1800-1810, 1984.

Reiners, A.J.H.M, E.B. Thornton, and T.C. Lippmann, Longshore currents over barred beaches, Coastal Dynamics, 413-424, 1995

Sallenger, A.H. and R.A. Holman, Wave energy saturation on a natural beach of variable slope, J. Gephys. Res., 90, 11939-11944, 1985.

Smith, J.M., M. Larson, and N.C. Kraus, Longshore current on a barred beach: Field measurements and calculation, J. Geophys. Res., v 98, 22,717- 22,731, 1993.

Symonds, G. and D.A. Huntley, Waves and currents over nearshore bar systems, Proc. Canadian Coastal Conf. Natl. Res. Council, Canada, 64-78, 1980.

Thornton, E.B, and R.T. Guza, Surf zone longshore currents and random waves: field data and models, J. Phys. Ocean., v 16 n 7, 1165-1178, 1986.

Thornton, E.B. and C.S. Kim, Longshore current and wave height modulation at tidal frequency inside the surf zone, J. Geophys. Res. v 98 16,509-16,519, 1993.

APPENDIX

In an operational setting it is not unusual that the staff oceanographic officer is tasked to provide a forecast of the surf conditions several days in the future. Offshore wave conditions can be derived from the atmospheric forecast models. The model as presented uses observed inputs of breaker height, breaker angle and surf zone width and there is no requirement for bathymetry. The data required to develop an empirical relationship between offshore wave height and surf zone width is not likely to be known. However, forward reconnaissance, surveillance activities, or archived data may provide an estimate of the beach slope.

Given this scenario, equations 5 and 6 can be reformulated to provide a prediction of the surf width (equation A1):

$$(A1) \qquad\qquad \hat{x}_b = \frac{H_s}{\gamma \tan \beta}$$

where $\hat{x}_b$ is the predicted surf zone width, H_s is the significant wave height, β is the beach slope, and γ is the breaker criterion given by equation 5 which is the ratio of the wave height to depth of water at breaking. If β is known and a value for γ is assumed, then the surf width can be determined. The sensitive factor in this formulation is the value of γ. For example, at Duck it has been shown to vary between 0.4 and 0.8 (Sallenger and Holman, 1985). Using these values, $\hat{x}_b$ varies from 125 meters ($\gamma = 0.4$) to 62.5 meters ($\gamma = 0.8$) when $\beta = 0.02$ and $H_s = 1$. So it is critical to have good estimate of the breaking criteria to estimate the surf width.